NJC

Accepted Manuscript

This is an *Accepted Manuscript*, which has been through the Royal Society of Chemistry peer review process and has been accepted for publication.

Accepted Manuscripts are published online shortly after acceptance, before technical editing, formatting and proof reading. Using this free service, authors can make their results available to the community, in citable form, before we publish the edited article. We will replace this *Accepted Manuscript* with the edited and formatted *Advance Article* as soon as it is available.

You can find more information about *Accepted Manuscripts* in the Information for Authors.

Please note that technical editing may introduce minor changes to the text and/or graphics, which may alter content. The journal's standard Terms & Conditions and the Ethical guidelines still apply. In no event shall the Royal Society of Chemistry be held responsible for any errors or omissions in this *Accepted Manuscript* or any consequences arising from the use of any information it contains.

ROYAL SOCIETY OF CHEMISTRY

www.rsc.org/njc

Ultrasensitive sensing tris (2, 3-dibromopropyl) isocyanurate based on the synergistic effect of amino and hydroxyl groups of molecularly imprinted poly (*o*-aminophenol) film

Xiuling Ma,[a] Jiaxiang Liu,[a] Dan Wu,[a] Lihua Wang,[a*] Zhangjing Zhang [a] and Shengchang Xiang [a, b*]

[a]*College of Chemistry and Chemical Engineering, Fujian Provincial Key Laboratory of Polymer Materials, Fujian Normal University, Fuzhou, Fujian, 350007,China.*
[b]*College of Life and Environmental Sciences, Minzu University of China, Beijing 100081, China.*
E-mail: scxiang@fjnu.edu.cn, lhwang@fjnu.edu.cn

Abstract: A facile approach for sensing an emerging persistent organic pollutants, tris(2,3-dibromopropyl) isocyanurate (TBC) is developed, based on coupling molecularly imprinting with electro-polymerization of *o*-aminophenol (OAP), which is electro-active monomers containing multifunctional groups. The poly-OAP film was deposited in an OAP solution by potentiodynamic cycling of potential with and without the template (TBC) on a glassy carbon electrode. Using $K_3[Fe(CN)_6]$ as an electro-active marker, the properties of the TBC imprinting electrode were investigated by electrochemical measurements. The results showed that the sensor with a low detection limit of 6.64×10^{-11} mol L^{-1} (*S/N*=3) for TBC determination was significantly different from the non-imprinted electrode. By selecting aniline without hydroxyl group as a reference for controlled trials, limit of detection for poly-OAP film-coated electrode is ca. 10 times smaller than that for polyaniline-coated one, and the sensitivities for poly-OAP film is ca. 2 times higher than that for polyaniline one. It demonstrated more binding sites might improve the detection ability of imprinted sensor.

Keywords：tris(2,3-dibromopropyl) isocyanurate; *o*-aminophenol; electro-polymerization; molecular imprinting; sensor

1 Introduction

The environmental chemistry of persistent organic pollutants (POPs) is fascinating areas of scientific research. [1] With the development of social demand and technology, emerging POPs were increasingly concerned by environmentalist. [2] A brominated flame retardant (BFR), hexabrominated heterocyclic tris-(2, 3-dibromopropyl) isocyanurate (TBC), an emerging POPs, was identified in the natural environment for the first time. [3] It is durable, thermally

stable, and resistant to water, photodegradation. It has been widely applied in polymer products for fire safety due to its excellent capability to reduce flammability. However, the rapidly increasingly levels of TBC lead to environmental problems. It was identified as one of the causative compounds inducing neuronal toxicity in the environmental samples by the neuronal toxicity-directed analysis. [4] Numerous studies showed that these chemicals are persistent, have long distance transport and bioaccumulative abilities, and may potentially harm ecosystems and human health. [5, 6] Several methods to detect TBC in environment were established including gas chromatography (GC) and liquid chromatography coupled with mass spectrometry (LC-MS). [4, 7] Zhao [8] and Feng [9] et al developed electrochemiluminescence (ECL) and photoelectrochemical immunosensor (PCI) techniques on the basis of a series of inorganic nanoparticles with good sensitivity and low detection limit. However, these protocols are either much complicated, or need relatively expensive equipments. Due to the low concentration in the environment, it is still an important but challenging task to develop a sensitive, rapid, convenient, and selective method for on-site determination of TBC.

Molecular imprinting, which was first proposed by Wulff et al [10] and much expanded by Mosbach et al, [11] has been proven to be a versatile avenue to afford the creation of specific recognition sites in synthetic polymers. [12-15] Molecular imprinting polymers (MIPs) are prepared by a process that involves co-polymerization of functional monomers and crosslinkers around template molecules. The molecules are removed from the polymer, rendering complementary binding sites capable of subsequent template molecule recognition. [16, 17] Compared to other recognition systems, MIPs with affinity and specificity possess many promising characteristics, such as desired selectivity, physical robustness, thermal stability, as well as low cost and easy preparation. Recently, MIPs have aroused extensive attention and widely applied in many fields, such as artificial enzymes, [18] solid-phase extraction, [19-21] chiral separation, [22] and ligand binding assays. [23, 24] Moreover, molecular imprinting technology offers considerable potential as a cost-effective alternative to the use of molecule-based recognition in a variety of sensor applications. [25-27] To satisfy the different detection purposes, imprinted sensor with well controlled physical forms have been developed through various fabrication methods. [28-31] Among these methods, electro-polymerization provides some advantages, for example, thickness control of the polymer layer that is crucial to the sensing of the analyte, ability to attach the sensor film to electrode surfaces of any shape and size, and compatibility with combinatorial and high-throughput approaches critical for the commercial development of molecular imprinting. [32-35]

In this paper, a strategy to incorporate molecule imprinting with electro-polymerization

of *o*-aminophenol (OAP), which is electro-active monomer containing multifunctional groups, is proposed to sense TBC, which is trace in water. Four electro-polymers with different monomers: OAP and aniline were prepared in presence (MIPs) or absence (NIPs) of TBC template molecule. OAP is chosen as the multifunctional monomer for electro-polymerization because of its ease to be electro-polymerized on various substrate materials to form films with good chemical and mechanical stability. [36, 37] Additionally, aniline lack of hydroxyl group is selected as a reference for controlled trials. Considering that TBC is electro-inactive over the studied potential range, an electro-active substance, hexacyanoferrate ($K_3[Fe(CN)_6]$), is chosen as the redox probe of the film coated electrodes in solutions. The experiments show that there is almost no response to both NIP electrodes, while the current of two MIP electrodes show the linear proportional to the TBC concentration within the measured range from amperometric *i-t* curve. What's more, the poly-OAP film-coated electrode with a low detection limit of 6.64×10^{-11} mol L^{-1} (*S/N*=3) is ca. 10 times smaller than that for polyaniline-coated one, and the sensitivities for poly-OAP film is ca. 2 times higher than that for polyaniline one. The result might confirm that the cooperative utilization of amino and hydroxyl groups on the OAP could provide an efficient avenue to improve the detection limit and sensitivities of MIP sensor. Our research provides new insight to construct the molecularly imprinting electro-polymers to ultrasensitively sense the trace POPs.

2 Experimental

2.1 Instruments and reagents

Morphology of the imprinted and non-imprinted films was characterized by SEM (XL30ESEM-TMP, Holland). A CHI660E electrochemical workstation (CHI Instrument, shanghai Chenhua Apparatus Company, China) was used for electrochemical measurements.

Tris(2,3-dibromopropyl) isocyanurate (TBC, purity > 97%) was purchased from TCI (Tokyo, Japan). *O*-aminophenol (OAP, chemically pure) was obtained from Sinopharm Chemical Reagent Co., Lid. All the other chemicals were analytical reagent grade or better.

2.2 Preparation of MIP sensor

Prior to modification, the GCE was polished with emery paper and chamois leather containing 0.3 μm and 0.05 μm Al_2O_3 slurry, respectively, and then thoroughly rinsed ultrasonically with ethanol, and doubly distilled water for 3 min in turn. Then the electrode was cycled between −0.3 V and 1.5 V in 0.5 mol L^{-1} H_2SO_4 at 100 mV/s scan rate that reproducible voltammogram was obtained.

TBC imprinting Poly-OAP-modified GCE (MIP sensor) was prepared (shown in Fig. 1)

by the following descriptions: the OAP solution was obtained by dissolving 0.0136 g OAP in 0.1 mol L^{-1} $HClO_4$, adjusting pH to 6 with 0.4 mol L^{-1} NaOH, and then diluted to 50 mL with water. The electro-polymerization solution was obtained by 20 mL OAP solution and 10 mL 1.0×10^{-4} mol L^{-1} TBC acetonitrile solution. Potentiodynamic cycling of potential for 30 scans in the range from -0.2~1.0 V was conducted at a scan rate of 50 mV/s. The sensor was rinsed with 0.5 mol L^{-1} H_2SO_4 for several times to remove TBC from the polymer matrix after electro-polymerization. The non-imprinted polymer sensor (NIP sensor) was also prepared in the same manner but without adding the template.

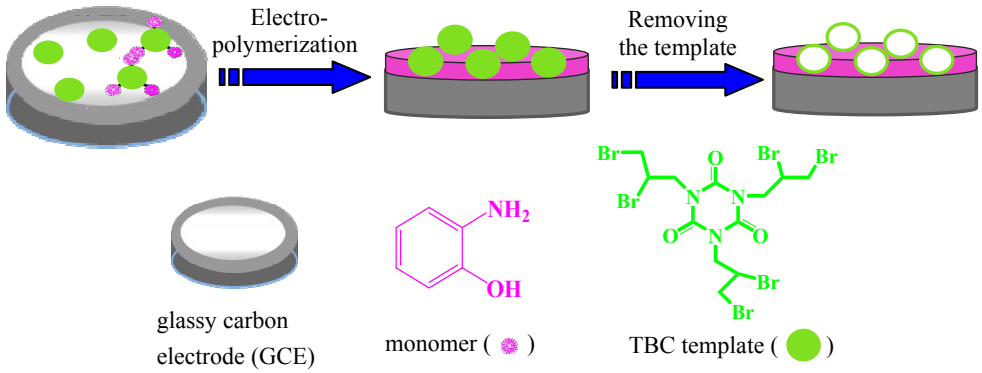

Fig. 1 Schematic diagram for the fabrication process of TBC imprinting OAP sensor

2.3 Measurements

A conventional three-electrode system was employed with a modified glassy carbon electrode (GCE, 3.0mm in diameter) as the working electrode, a platinum electrode as the counter electrode, and an Ag/AgCl electrode with saturated KCl as the reference electrode. All potentials reported in this article were referenced to the Ag/AgCl electrode. All measurements were carried out at room temperature.

The AC (potential: 0 V) was utilized to evaluate the effect of the groups of functional monomers on the detection limit of the sensors and response to different substances. The electrochemical performance of different sensors was studied by cyclic voltammetry (CV) and electrochemical impedance spectroscopy (EIS). Differential pulse voltammetry (DPV) was used to examine the degree of removing TBC molecules and imprinting effect. CV, DPV, EIS and amperometric *i-t* curve experiments were performed in the 10 mL 5.0 mmol L^{-1} background solution $K_3[Fe(CN)_6]$ with adding 0.1 mol L^{-1} KCL as support electrolyte. The potential range of CV was taken from -0.2 V to 0.6 V at 20 mV/s. Current measurements were performed using DPV in a potential range between -0.2 V and 0.6 V, a modulation amplitude of 50 mV, a pulse width of 100 ms and a step potential of 5 mV.

3 Results and discussion

3.1 Preparation of MIP sensor

3.1.1 Electro-polymerization

In this work, the electro-polymerization of OAP was employed to prepare the sensitive film of MIP sensor with uniform and controlled thickness. As shown in Fig. 2, in the first cycle, OAP oxidizes to radical cation (peak A1) , and follow-up reactions give products detected as peak A2/A3 on the subsequent sweeps, attributed to species in solution and deposited on the electrode surface, respectively. [38] Current of peak A1, A2 and A3 slow down with increasing the cycles. Such a trend has been justified in terms of hindered diffusion of the relative redox species to the electrode upon the formation of a layer on the electrode surface. The growing film, indeed, is reported to be non-conducting in its fully oxidative state and then itself unable to oxidize the monomer. As for molecularly imprinted polymer, the applications of poly-OAP take advantage of the formation of hydrogen bonds between the templates and $–NH_2$ and –OH groups present along the polymer skeleton. [39]

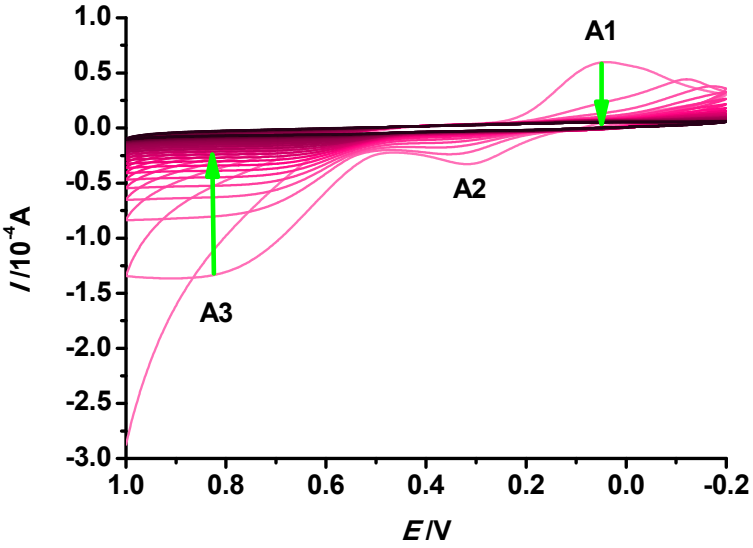

Fig. 2 CV during the electro-polymerization of OAP

3.1.2 Elution

Removing the imprinting molecular is an important factor when preparing MIPs. The imprinted cavities matched with the imprinting molecule will be formed after eluting the temple molecule. [11] Fig. 3 shows MIP electrode before elution (curve c) and NIP electrode (curve d) didn't appear the $K_3[Fe(CN)_6]$ peak current response, while the value of peak current of MIP electrode after elution (curve b) is near to the bared electrode (curve a). Due to the dense films coated on the surface of MIP electrode before elution or NIP electrode, there was

no electrochemical reaction occurred. During eluting, the interaction between the OAP and TBC would be destroyed under the condition of strong acidity, which resulted in the leakage of TBC molecules from the stereoscopic cavity of the imprinted film. Electrochemical reaction was occurred by $[Fe(CN)_6]^{3-}$ ion through the imprinted cavities into the MIP electrode surface, while NIP electrode couldn't. The differences between NIP electrode and MIP electrode after elution (MIP sensor) were illustrated by various characterizations in the later section.

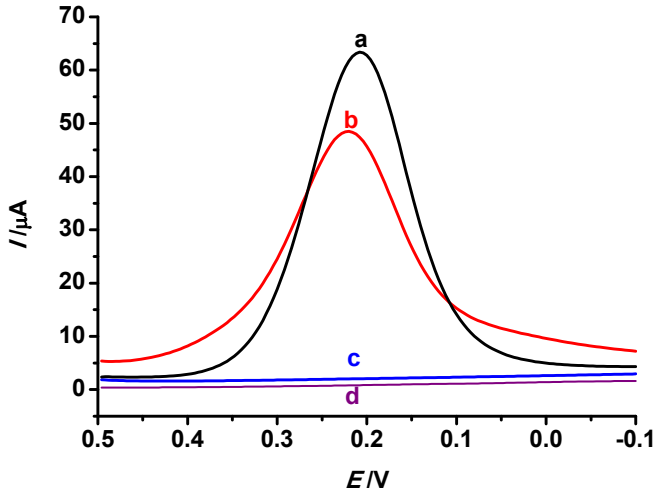

Fig. 3 DPV of bared/MIP/NIP sensors using OAP as functional monomer (a: bared electrode; b: MIP electrode after elution; c: MIP electrode before elution; d: NIP electrode)

3.1.3 Characterization of MIP/NIP sensors

3.1.3.1 The morphologies

The morphologies of MIP/NIP sensors using OAP as functional monomer were observed by SEM as shown in Fig. 4. The surface morphology of NIP sensor or MIP sensor before elution is compact, after the template extraction, the imprinted sensor becomes rough, probably caused by the change of macroscopic porosity of the MIP after the analyte extraction. During the imprinting process, channels can be generated by template molecules increasing the fraction of microspores in the polymer while also producing structures, complementary to that of the template. [40]

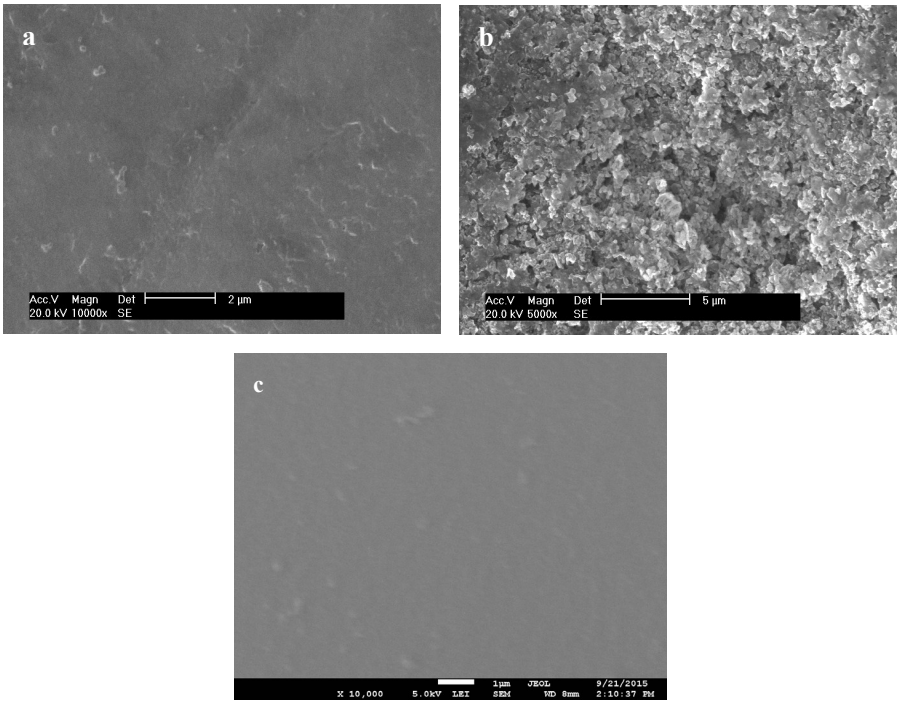

Fig. 4 SEM photographs (a): NIP sensor, (b): MIP sensor after elution, (c): MIP sensor before elution using OAP as functional monomer

3.1.3.2 Electrochemical properties of sensors

The electrochemical properties of different sensors were studied by CV (Fig. S1). To MIP sensor, a pair of obvious oxidation and reduction peak attributed to the redox reaction of $[Fe(CN)_6]^{3-}$ ion was observed, and consistent with that of the bare electrode, however, no redox peak in the NIP electrode. This is mainly because $[Fe(CN)_6]^{3-}$ ion is largely blocked from diffusing to the electrode by the dense surface structure of NIP electrode**.** After removing the imprinting molecule, a lot of irregular cavities were formed on the surface of the MIP sensor. Thus the oxidation-reduction reaction could take place when $[Fe(CN)_6]^{3-}$ ion diffused to an electrode surface through the cavities.

EIS is an efficient tool for studying the interface properties of surface-modified electrodes. To further characterize the surface property of the sensors, EIS (Init E=0 V、High Freq= 1×10^4 Hz、Low Freq=1 Hz、Amplitude=0.005 V) was used to investigate the charge transfer resistance of the film. As shown in Fig. 5, by fitting the semicircle portion corresponds to the electron transfer-limited process, the electron transfer resistance (R) at electrode surface are 608, 6652, and 18468 Ω, respectively. The result manifests that the imprinted one had a lower electron transport barrier presumably due to the existence of porous binding sites after the template removal. The decrease in interfacial impedance is desirable because it can decrease both the interfacial resistance drop of the electrode current

and overpotential, leading to the enhancement of sensorial sensitivity.

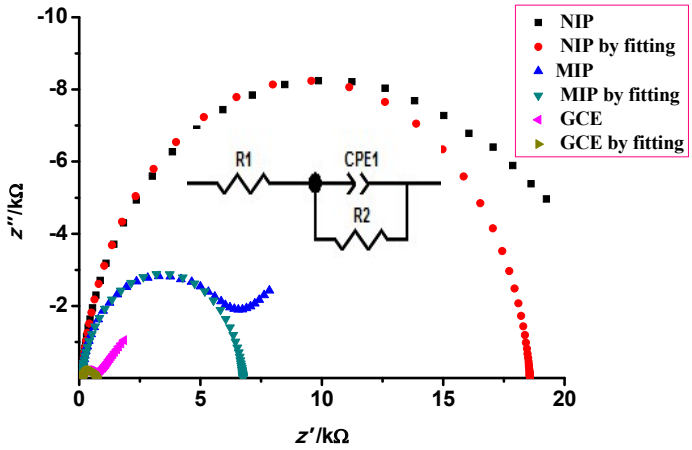

Fig. 5 Nyquist plots and fitting plots of MIP/NIP electrodes using OAP as functional monomer

The influence of scan rate on the MIP sensor was also investigated by CV (Fig. S2), the peak current increased with the scan rate over the range of 20 mV/s ~250 mV/s and a good linear relationship between the anodic peak current and the square root of scan rates ($v^{1/2}$) was obtained. The regression equation was I_{pa} = -4.644 $v^{1/2}$ - 15.04 with a correlation coefficient of 0.97195. Moreover, the cathodic peak current was strongly dependent on the scan rate and the regression equation was I_{pc} = 2.172 $v^{1/2}$ +14.60 with a correlation coefficient of 0.98198. This indicated the reaction of imprinted sensor is a typical diffusion controlling process.

3.2 Performance of the MIP sensor

3.2.1 Effect of imprinting

In this study, DPV was employed for the quantitative determination of TBC, which is relatively sensitive compared to the conventional CV method. DPV was performed after the MIP sensor was immersed in solutions containing TBC of different concentration (1.0×10^{-10}, 1.0×10^{-9}, 1.0×10^{-8} mol L^{-1}) and the background solution (5 mmol L^{-1} $K_3[Fe(CN)_6]$ solution). When the MIP sensor was immersed in the solution containing TBC, the cavities in the film were partially occupied by TBC, which led to the decrease of current signal produced by $[Fe(CN)_6]^{3-}$. As shown in Fig. 6, the higher the concentration of TBC, the lower the current would be, which suggests that more and more binding sites in the film are occupied by TBC molecules.

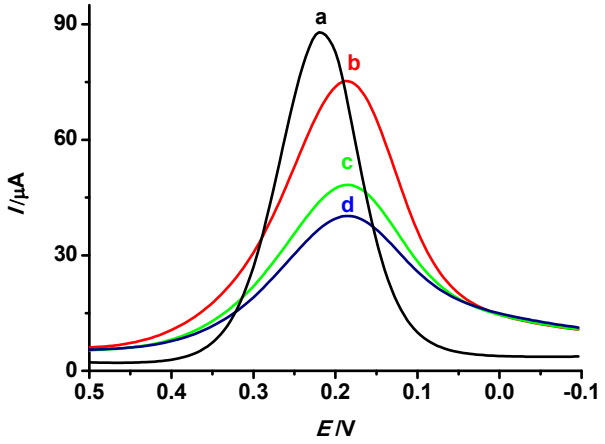

Fig. 6 DPV responses of TBC imprinting OAP sensor to the different concentration of TBC (a: 0, b: 1.0×10^{-10} mol L^{-1}, c: 1.0×10^{-9} mol L^{-1}, d: 1.0×10^{-8} mol L^{-1})

3.2.2 The detection limit of the sensors

In order to evaluate the detection limit of sensors which was obtained from the change of reduction current of $K_3[Fe(CN)_6]$, measurements of amperometric *i-t* curve were performed in the 7 mL 5 mmol L^{-1} $K_3[Fe(CN)_6]$ solution, and 0.1 mL 1.0×10^{-8} mol L^{-1} TBC was added in it every the same time. The reduction peak current of $K_3[Fe(CN)_6]$ gradually decreased with increasing TBC concentrations (Fig. 7A, curve a). It appeared a platform at every concentration stage and stability in 30 s, which indicated that the MIP sensor has short response time. However, there was almost no response to NIP electrode (Fig. 7A, curve b). When MIP electrode sensor was immersed into the mixture solution, TBC molecules could be absorbed because of the imprinting spatial similarity. Therefore, it causes the variation of the $K_3[Fe(CN)_6]$ peak current response. The result showed that the recognition sites of TBC were formed in the MIP sensor, which played an important role in the process of recognition. The relative change of the peak current is linearly proportional to the TBC concentration in the range of 1.4×10^{-10} mol L^{-1} to 6.7×10^{-10} mol L^{-1} (shown in Fig. 7A inset), with a correlation coefficient of 0.99029. The usable linear concentration range is limited, however, the limit of detection (LOD, *S/N*=3) was 6.64×10^{-11} mol L^{-1}, which was more significantly outperformed than the sensor constructed by ECL [8] and equivalent to PCI. [9] The sensitivity of the sensor is 3.275×10^{4} A/(mol L^{-1}).

Aniline, another functional monomer, was chosen as a reference. The sensors were prepared by the same operation for OAP. The morphologies of MIP sensors were observed by SEM in Fig. S3. The detection limit of the imprinted sensor was obtained as the same method

of OAP. As shown in Fig. 7B inset, the relative change of the peak current is linearly proportional to the TBC concentration in the range of 1.96×10^{-10} mol L^{-1} to 9.09×10^{-10} mol L^{-1}, with a correlation coefficient of 0.99679. The LOD (S/N=3) of imprinted aniline sensor was 5.22×10^{-10} mol L^{-1}, which was higher than the imprinted OAP sensor. And the sensitivity of the sensor is 1.621×10^{4} A/(mol L^{-1}), lower than OAP's. OAP can bind to TBC probably via O-H…O and N-H…O hydrogen bonds, which facilitates the recognition and selectivity for the analyte (shown in Fig. 8). That is, the cooperative utilization of amino and hydroxyl groups on the OAP could improve the detection limit of MIP sensor. The MIP sensor we proposed is desirable for the detection of trace amounts TBC in environmental samples.

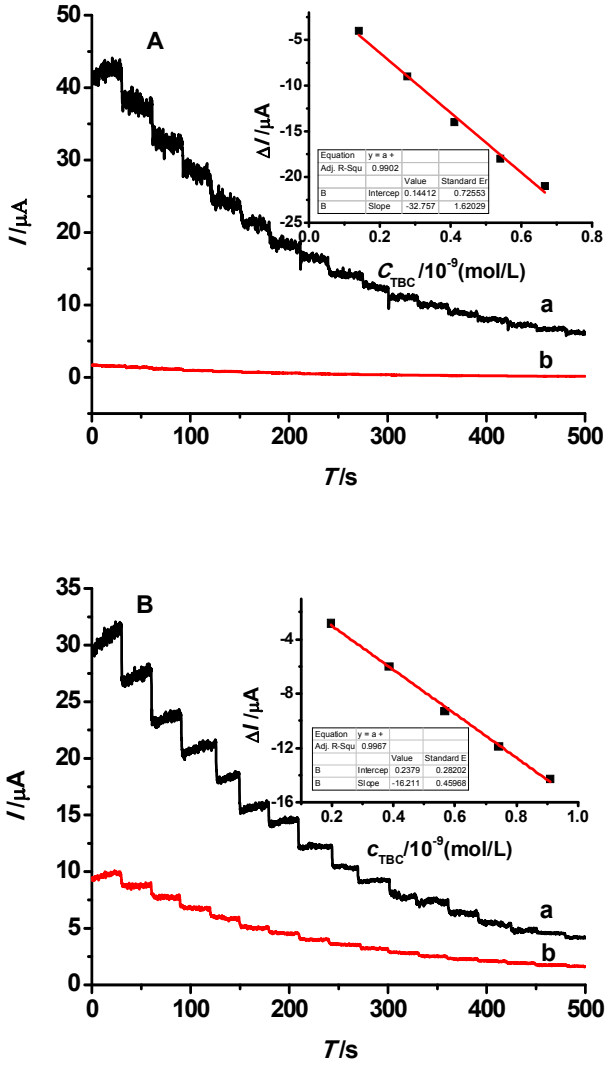

Fig. 7 Amperometric *i-t* curve of the sensors (a: MIP sensor, b: NIP sensor; A: OAP as the functional monomer, the added concentration of TBC is 0, 1.40×10^{-10}, 2.78×10^{-10}, 4.11×10^{-10}, 5.41×10^{-10}, 6.67×10^{-10} mol L^{-1}, and so on; B: aniline as the functional monomer, the added concentration of TBC is 0, 1.96×10^{-10}, 3.85×10^{-10}, 5.66×10^{-10}, 7.41×10^{-10}, 9.09×10^{-10} mol L^{-1},

and so on), inset shows the linear relation of $\triangle I \sim C_{TBC}$)

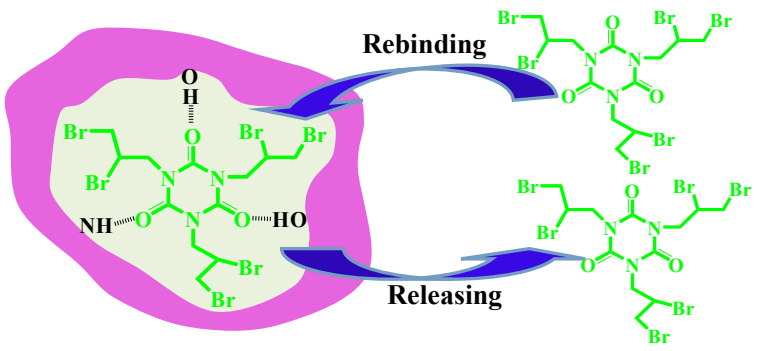

Fig. 8 Schematic diagram for the interaction of TBC and OAP

3.2.3 The recognition performance of MIP sensor

In order to investigate the recognition performance of MIP sensor, two species, phenol and melamine were employed as interference for selectivity tests by amperometric *i-t* curve with the same operation as the test of detection limit. As shown in Fig. 9, under the same operation condition, the MIP sensor shows similar response to the structural analogues: melamine and TBC, but no response to phenol. Melamine and TBC have the same triazine ring structure. The sensitivity toward melamine is 3.200×10^4 A/(mol L^{-1}) (Figure S4), just slightly lower than that for TBC. The removal of the template, in fact, allows generating molecular cavities with recognizing sites toward structural analogues.[41] Therefore, melamine has a chance of approaching the imprinting sites. Furthermore, the current value of TBC is always lower than melamine or phenol. TBC bound to the polymer film, occupied the binding sites and blocked the reduction of the ferricyanide species, therefore much lower currents have been observed as in the case of the $K_3[Fe(CN)_6]$ solution. Based on the interaction between the template and the imprinting sites, MIPs have selectivity towards the template molecule and its analogues. The recognition sites formed in the polymerized film have the capability to distinguish target molecules through their size, shape and functional group distribution.[42]

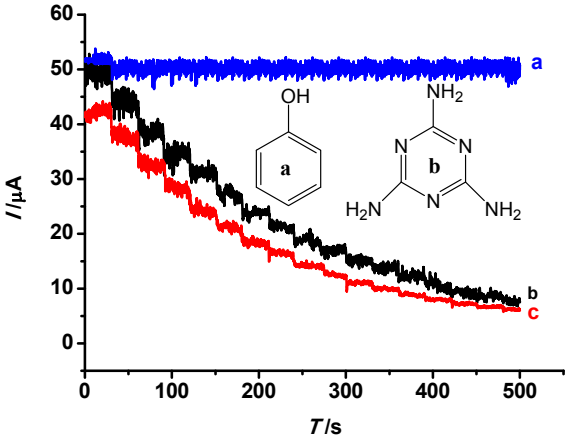

Fig. 9 AC response of the imprinted OAP sensor to different substances ((a: phenol; b: melamine; c: TBC, the added concentration of different substances is 0, 1.40×10^{-10}, 2.78×10^{-10}, 4.11×10^{-10}, 5.41×10^{-10}, 6.67×10^{-10} mol L^{-1}, and so on)

3.2.4 The regeneration of MIP sensor

Regeneration is one of the most important properties for the application of the imprinted sensor. Therefore, the sensor was immersed in 0.5 mol L^{-1} H_2SO_4 solution for 2 h with ultrasonic oscillation, and back to the initial status. DPV was applied in the solutions containing 5 mmol L^{-1} $K_3[Fe(CN)_6]$ or 5 mmol L^{-1} $K_3[Fe(CN)_6]$ and 1.0×10^{-8} mol L^{-1} TBC. The cycle was repeated using the above description. As shown in Tab. 1, the value of current with or without TBC did change, but not much. A relative standard deviation (RSD) is 1.76% for three times, which indicates excellent regeneration performance.

Table 1. The regeneration of OAP imprinting sensor

Number	I/μA (without TBC)	I/μA（adding TBC）	ΔI/μA
1	164.8	114.2	50.6
2	164.8	115.9	48.9
3	152.5	103.1	49.4

4 Conclusions

To determine ultra-trace TBC, a new approach for the fabrication of the TBC-MIP sensor was presented. The modified electrode exhibited a low detection limit (6.64×10^{-11} mol L^{-1}) and good recognition performance. Sensitivity and regeneration were achieved by combining a molecular imprinting technique and the electrochemistry of a poly (*o*-aminophenol) film on the GCE. In addition, the fabrication procedure is very simple, rapid, and inexpensive. The

poly (*o*-aminophenol) based MIP electrode, in comparison with the polyaniline one with less binding sites, shows improved detection ability. We believe that our strategy is instructive to the determination of other POPs molecules, which is insoluble in water, and non-electrochemical activities.

Acknowledgments

This work was financially supported by the National Natural Science Foundation of China (21207018, 21273033 and 21203024), Natural Science Foundation of Fujian Province (2015J01039, 2014J06003, 2014H6007) and Fujian Education Department (JA13061). S. X. gratefully acknowledges the supports from Recruitment Program of Global Young Experts, Program for New Century Excellent Talents in University (NCET-10-0108), and the Award 'MinJiang Scholar Program' in Fujian Province.

Notes and references

1 K. C. Jones and P. de Voogt, *Environ. Pollut*., **1999**, 100, 209.

2 L. Dong, X. L. Zhang, S. X. Shi, P. J. Xue, L. Zhou, W. L. Yang, L. F. Zhang, T. Zhang and Y. R. Huang, *Sci. China-chem.*, **2013**, 43, 336.

3 T. Ruan, Y. W. Wang, C. Wang, P. Wang, J. J. Fu, Y. G. Yin, G. B. Qu, T. Wang and G. B. Jiang, *Environ. Sci. Technol.*, **2009**, 43, 3080.

4 G. B. Qu, J. B. Shi, Z. N. Li, T. Ruan, J. J. Fu, P. Wang, T. Wang and G. B. Jiang, *Sci. China-chem.*, **2011**, 54, 1651.

5 L. S. Birnbaum and D. F. Staskal, *Environ. Health Perspect.*, **2004**, 112, 9.

6 J. Li, Y. Liang, X. Zhang, J. Y. Lu, J. Zhang, T. Ruan, Q. F. Zhou and G. B. Jiang, *Environ. Sci. Technol.*, **2011**, 45, 9750.

7 D. C. G. Muir and P. H. Howard, *Environ. Sci. Technol.*, **2006**, 40, 7157.

8 P. Zhao, G. M. Cao, L. F. Zhou, Q. Liu, M. L. Guo, Y. Huang, Q. Y. Cai and S. Z. Yao, *Analyst*, **2011**, 136, 1952.

9 H. Feng, L. P. Zhou, J. Z. Li, T. T. Tran. T, N. Wang, L. J. Yuan, Z. H. Yan and Q. Y. Cai *Analyst*, **2013**, 138, 5726.

10 G. Wulff and A. Sarhan, *Angew. Chem., Int. Ed. Engl.*, **1972**, 11, 341.

11 L. Andersson, B. Sellergren and K. Mosbach, *Tetrahedron Lett*., **1984**, 25, 5211.

12 Y. Liu, Y. Gu, M. Li and Y Wei, *New J. Chem*., **2014**, 38, 6064.

13 L. Ye and K. Mosbach, *Chem. Mater.*, **2008**, 20, 859.

14 Q. Osmani, H. Hughes and P. McLoughlin, *J. Mater. Sci*., **2012**, 47, 2218.

15 X. L. Ma, J. X. Liu, Z. J. Zhang, L. H. Wang, Z. Chen and S. C. Xiang, *RSC Adv.*, **2013**, 3, 25396.

16 D. Cai, L. Ren, H. Z. Zhao, C. J. Xu, L. Zhang, Y. Yu, H. Z. Wang, Y. C. Lan, M. F. Roberts, J. H. Chuang, M. J. Naughton, Z. F. Ren and T. C. Chiles, *Nat. Nanotechnol.*, **2010**, 5, 597.

17 L. Chen, S. Xua and J. Lia, *Chem. Soc. Rev.*, **2011**, 40, 2922.

18 F. Bonini, S. Piletsky, A. P. F. Turner, A. Speghini and A. Bossi, *Biosens. Bioelectron*., **2007**, 22, 2322.

19 S. Chen, Z. M. Luo, X. L. Ma, L. Q. Xue, H. X. Lan and W. B. Zhang, *Anal. Lett.,* **2012,** 45, 2300.

20 F. Augusto, L. W. Hantao, N. Mogollon and S. Braga, *Trac-trends Anal. Chem.*, **2013**, 43, 14.

21 Z. R. Lian and J. T. Wang, *Environ. Pollut*., **2013**, 182, 385.

22 V. B. Kumar, Y. Mastai, Z. Porat and A. Gedanken. *New J. Chem.,* **2015,** 39, 2690.

23 E. Benito-Pena, M. C. Moreno-Bondi, S. Aparicio, G. Orellana, J. Cederfur and M. Kempe, *Anal. Chem*., **2006**, 78, 2019.

24 Y. Ma, G. Q. Pan, Y. Zhang, X. Z. Guo and H. Q. Zhang, *Angew. Chem., Int. Ed.,* **2013**, 52, 1511.

25 V. K. Gupta, M. L. Yola and N. Atar, *Sensor Actuat. B-Chem*., **2014**, 194, 79.

26 P. N. Zhao and J. C. Hao, *Food Chem.*, **2013**, 139, 1.

27 T. P. Huynh, B. K. C Chandra, M. Sosnowska, J. W. Sobczak, V. N. Nesterov, F D'Souza and W. Kutner, *Biosens. Bioelectron.*, **2015**, 64, 657.

28 B. Rezaei, O. Rahmanian and A. A. Ensafi, *Sensor Actuat. B-Chem*., **2014**, 196, 539.

29 T. S. Anirudhan and S. Alexander, *Biosens. Bioelectron.*, **2015**, 64, 586.

30 X. Wang, X. Li, C. Luo, M. Sun, L. Li and H. Duan, *Electrochim. Acta,* **2014**, 130, 519.

31 R. N. Liang, D. A. Song, R. M. Zhang and W. Qin, *Angew. Chem. Int. Ed.*, **2010**, 49, 2556.

32 R. Pernites, R. Ponnapati, M. J. Felipe and R. Advincula, *Biosens. Bioelectron.*, **2011**, 26, 2766.

33 S. Li, J. Luo, G. Yin, Z. Xu, Y. Le, X. Wu, N. Wu and Q. Zhang, *Sensor Actuat. B-Chem*., **2015**, 206, 14.

34 V. K. Gupta, M. L. Yola, N. Özaltın, N. Atar, Z. Üstünda and L. Uzun, *Electrochim. Acta.*, **2013**, 112, 37.

35 A. Turco, S. Corvaglia and E. Mazzotta, *Biosens. Bioelectron*., **2015**, 63, 240.

36 Rosy, H. Chasta and R. N. Goyal, *Talanta*, **2014**, 125, 167.

37 F. T. C. Moreira, S. Sharma, R. A. F. Dutra, J. P. C Noronha, A. E. G. Cass and M. G. F. Sales, *Sensor Actuat. B-Chem*., **2014**, 196, 123.

38 R. Tucceri, P. M. Arnal and A. N. Scian, *ISRN Polymer Science,* **2012**, doi:10.5402/2012 /942920.

39 M. E. Carbone, R. Ciriello, S. Granafei, A. Guerrieri and A. M. Salvi, *Electrochim. Acta*, **2014**, 144, 174.

40 S. A. Piletsky, T. L. Panasyuk, E. V. Piletskaya, I. A. Nicholls and M. Ulbricht, *J. Membr. Sci.*, **1999**, 157, 263.

41 J. Matsui, K. Fujiwara and T. Takeuchi, *Anal. Chem.*, **2000**, 72, 1810.

42 Y. T. Liu, J. Deng, X. L. Xiao, L. D., Y. L. Yuan, H. Li, X. T. Li, X. N. Yan and L. L. Wang. *Electrochim. Acta*, **2011**, 56, 4595.

Table of Contents

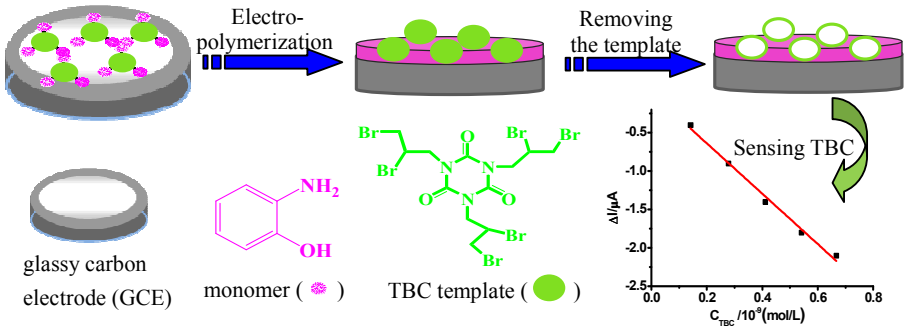

Ultrasensitive sensing tris(2,3-dibromopropyl) isocyanurate was achieved by the synergistic effect of amino and hydroxyl groups in imprinted poly(*o*-aminophenol) film.